Kinetic and Mechanistic Aspects of Propene Oligomerization with Ionic Organozirconium and -hafnium Compounds: Crystal Structures of $[Cp^*_2MMe(THT)]^+[BPh_4]^-$ (M = Zr, Hf)[1]

Johan J. W. Eshuis, Yong Y. Tan, Auke Meetsma, and Jan H. Teuben*

Groningen Center for Catalysis and Synthesis, Department of Chemistry, University of Groningen, Nijenborgh 16, 9747 AG Groningen, The Netherlands

Jaap Renkema and George G. Evens

DSM Research BV, P.O. Box 18, 6160 MD Geleen, The Netherlands

Received August 23, 1991

In *N,N*-dimethylaniline the ionic complexes $[Cp^*_2MMe(THT)]^+[BPh_4]^-$ (M = Zr, Hf) oligomerize propene to low molecular weight oligomers. At room temperature for M = Zr a rather broad molecular weight distribution is obtained (C_6 to C_{24}), whereas for M = Hf only one dimer (4-methyl-1-pentene) and one trimer (4,6-dimethyl-1-heptene) are formed. With an increase in reaction temperature the product composition shifts to lower molecular weights, but the specific formation of head-to-tail oligomers is retained. The oligomers are formed by β-Me transfer from the growing oligopropene alkyl chain to the metal center. The molecular weight distributions of the oligomers produced at temperature between 5 and 45 °C are satisfactorily described by the Flory–Schulz theory. This allows the calculation of ratios of rate coefficients for propagation (k_p) and termination (k_t). Values for $(\Delta G^{\ddagger}_p - \Delta G^{\ddagger}_t)_{298K}$ were calculated as −1.9 (3) and −1.4 (4) kcal·mol^{-1} for $[Cp^*_2ZrMe(THT)]^+[BPh_4]^-$ and $[Cp^*_2HfMe(THT)]^+[BPh_4]^-$, respectively. Both complexes crystallize in the space group $Pna2_1$ with a = 31.31 (1) Å, b = 11.844 (4) Å, c = 11.084 (4) Å, V = 4110 (2) Å^3, and Z = 4 for $[Cp^*_2ZrMe(THT)]^+[BPh_4]^-$ and a = 31.32 (1) Å, b = 11.857 (1) Å, c = 11.029 (1) Å, V = 4096 (1) Å^3, and Z = 4 for $[Cp^*_2HfMe(THT)]^+[BPh_4]^-$. A molecular modeling study based on the molecular structures using the ALCHEMY software package suggests that the conformations with the β-Me group in the plane between the Cp* rings are more stable than the conformations with the β-Me group pointing toward one of the Cp* ligands. Inactivation of the catalysts is caused by two different mechanisms. At room temperature allylic C–H activation of monomer and isobutene (formed by a minor β-H transfer termination) gives inactive (meth)allyl compounds, $[Cp^*_2M(\eta^3\text{-}C_3H_5)]^+$ and $[Cp^*_2M(\eta^3\text{-}C_4H_7)]^+$ (M = Zr, Hf). At elevated temperatures (>45 °C) catalytically inactive zwitterionic complexes $Cp^*_2M^+\text{-}m\text{-}C_6H_4\text{-}BPh_3^-$ (M = Zr, Hf) are formed through aromatic C–H activation. Reactivation of the inactive (meth)allyl complexes can be achieved by addition of hydrogen to the oligomerization mixtures.

Introduction

Neutral d^0f^n, 14-electron complexes Cp^*_2LnR (Ln = lanthanide or group 3 metal, R = alkyl, H) and cationic d^0, 16-electron complexes $[Cp^{\dagger}_2MR(L)]^+$ ($Cp^{\dagger} = \eta^5\text{-}C_5H_{5-n}Me_n$, n = 0, 1, 5, M = group 4 metal, L = Lewis base, R = alkyl, H) have raised considerable interest with regard to catalytic olefin oligomerization and polymerization.[2,3] Compounds of the type $[Cp^*_2LnH]_2$ rank among the most active homogeneous catalysts for the polymerization of ethene known to date.[4] The activity toward higher α-olefins seems to be largely determined by steric factors. Whereas Cp^*_2ScR (R = alkyl) compounds are good catalysts for the polymerization of ethene[5] and have been used as well-defined, single-component model systems for Ziegler–Natta polymerizations,[2g] catalytic activity toward higher α-olefins (dimerization) and α,ω-dienes (cyclization/branching) is only observed for scandium compounds in which the coordination sphere around the metal center has been enlarged using bridged dicyclopentadienyl ligands $Me_2Si(C_5Me_4)_2$ or $Me_2Si(C_5H_3{}^tBu)_2$.[2f,5b]

One of the most striking features of a number of catalytic systems based on Cp^*_2MR (M = Lu, R = alkyl), $[Cp^*_2MMe(THT)]^+$ (M = Zr, Hf), and $Me_2Si(^tBuC_5H_3)_2ScR$ (R = hydride) is their propensity to terminate chain growth by β-alkyl elimination[2b,c,f,4,6] instead of the more commonly encountered β-H elimination.[7]

Our group has focused on the more fundamental aspects of the initiation, propagation, and termination steps in olefin oligomerization and polymerization with ionic group 4 complexes $[Cp^*_2MMe(THT)]^+[BPh_4]^-$ (M = Ti, Zr, Hf). We have shown that these compounds (M = Zr, Hf) are effective catalysts for the polymerization of ethene and that

(1) In this paper the following abbreviations are used: Cp = η^5-C_5H_5, Cp′ = η^5-C_5H_4Me, Cp* = η^5-C_5Me_5, THT = tetrahydrothiophene.

(2) For leading references, see: (a) Watson, P. L. *J. Am. Chem. Soc.* **1982**, *104*, 337. (b) Watson, P. L.; Roe, D. C. *J. Am. Chem. Soc.* **1982**, *104*, 6471. (c) Watson, P. L.; Parshall, G. W. *Acc. Chem. Res.* **1985**, *18*, 51. (d) Jeske, G.; Lauke, H.; Mauermann, H.; Swepston, P. N.; Schumann, H.; Marks, T. J. *J. Am. Chem. Soc.* **1985**, *107*, 8091. (e) Thompson, M. E.; Baxter, S. M.; Bulls, A. R.; Burger, B. J.; Nolan, M. C.; Santarsiero, B. D.; Schaefer, W. P.; Bercaw, J. E. *J. Am. Chem. Soc.* **1987**, *109*, 203. (f) Bunel, E.; Burger, B. J.; Bercaw, J. E. *J. Am. Chem. Soc.* **1988**, *110*, 976. (g) Burger, B. J.; Thompson, M. E.; Cotter, W. D.; Bercaw, J. E. *J. Am. Chem. Soc.* **1990**, *112*, 1566.

(3) For leading references, see: (a) Bochmann, M.; Wilson, L. M. *J. Chem. Soc., Chem. Commun.* **1986**, 1610. (b) Jordan, R. F.; Bajgur, C. S. *J. Am. Chem. Soc.* **1986**, *108*, 7410. (c) Jordan, R. F.; LaPointe, R. E.; Bajgur, C. S.; Echols, S. F.; Willett, R. *J. Am. Chem. Soc.* **1987**, *109*, 4111. (d) Bochmann, M.; Wilson, L. M.; Hursthouse, M. B.; Short, R. L. *Organometallics* **1987**, *6*, 2556. (e) Jordan, R. F. *J. Chem. Educ.* **1988**, *65*, 285. (f) Hlatky, G. G.; Turner, H. W.; Eckman, R. R. *J. Am. Chem. Soc.* **1989**, *111*, 2728. (g) Jordan, R. F.; LaPointe, R. E.; Bradley, P. K.; Baenziger, N. *Organometallics* **1989**, *8*, 2892. (h) Bochmann, M.; Jaggar, A. J.; Wilson, L. M.; Hursthouse, M. B.; Motevalli, M. *Polyhedron* **1989**, *8*, 1838. (i) Jolly, C. A.; Marynick, D. S. *J. Am. Chem. Soc.* **1989**, *111*, 7968. (j) Christ, C. S., Jr.; Eyler, J. R.; Richardson, D. E. *J. Am. Chem. Soc.* **1990**, *112*, 596. (k) Jordan, R. F.; Taylor, D. F.; Baenziger, N. C. *Organometallics* **1990**, *9*, 1546. (l) Park, J. W.; Henling, L. M.; Schaefer, W. P.; Grubbs, R. H. *Organometallics* **1990**, *9*, 1650.

(4) (a) Watson, P. L.; Herskovitz, T. In *Initiation of Polymerization*; Bailey, Jr., Ed.; ACS Symposium Series 212; American Chemical Society: Washington, DC, 1983; Chapter 32. (b) Kaminsky, W.; Lüker, H. *Makromol. Chem., Rapid Commun.* **1984**, *5*, 225.

(5) (a) Thompson, M. E.; Bercaw, J. E. *Pure Appl. Chem.* **1984**, *56*, 1. (b) Parkin, G.; Bunel, E.; Burger, B. J.; Trimmer, M. S.; Van Asselt, A.; Bercaw, J. E. *J. Mol. Catal.* **1987**, *41*, 21.

(6) Eshuis, J. J. W.; Tan, Y. Y.; Renkema, J.; Teuben, J. H. *J. Mol. Catal.* **1990**, *62*, 277.

(7) See for example: (a) Sinn, H.; Kaminsky, W. *Adv. Organomet. Chem.* **1980**, *18*, 99. (b) Kaminsky, W.; Ahlers, A.; Möller-Lindenhof, N. *Angew. Chem.* **1989**, *101*, 1304.

0276-7333/92/2311-0362$03.00/0

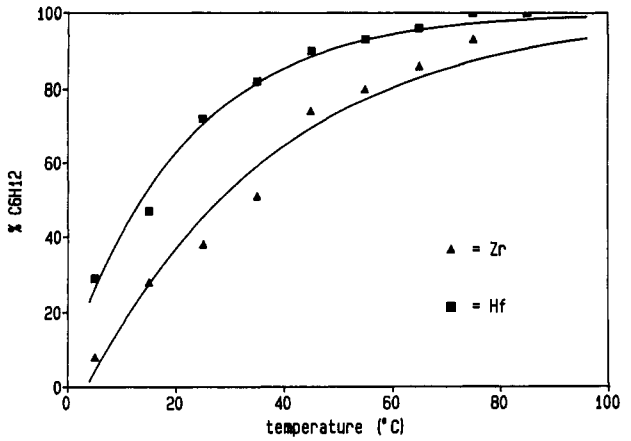

Figure 1. Plot of the selectivity of the propene dimerization for 1 and 2 against the temperature.

they oligomerize propene.[6] The catalytic systems show a remarkable difference in selectivity toward propene. Whereas the zirconium compound at room temperature produces oligomers up to C_{24}, the hafnium compound only gives one dimer (4-methyl-1-pentene) and one trimer (4,6-dimethyl-1-heptene) under the same conditions. Labeled propene CH_2=CH—CD_3 was used to demonstrate that β-Me elimination is the dominant termination which accounts for over 97% of the products obtained.[6] Termination of chain growth by β-H transfer to the metal takes place as well but is a minor pathway (<3%).

In this paper we report the effect of temperature on the initiation, propagation, and termination reactions and correlate the results to differences in activation parameters. Further, the inactivation of the catalysts was determined at various temperatures and methods developed to reactivate the catalysts.

Results and Discussion

Effect of Temperature on Oligomerization. Products. As described earlier,[6] both complexes $[Cp^*_2ZrMe(THT)]^+[BPh_4]^-$ (1) and $[Cp^*_2HfMe(THT)]^+[BPh_4]^-$ (2) oligomerize propene at room temperature in *N,N*-dimethylaniline. The Hf complex gives exclusively the dimer 4-methyl-1-pentene, and the trimer, 4,6-dimethyl-1-heptene. The Zr complex gives a much broader distribution with oligomers up to C_{24}. At higher temperatures the formation of the lower oligomers is clearly favored (Figure 1). This was especially evident for the hafnium compound, where above 55 °C the dimer 4-methyl-1-pentene forms more than 95% of the oligomerization products. For the zirconium-based catalyst this level of selectivity is not achieved within the temperature range studied. At lower temperatures broad distributions are obtained for both the Zr and Hf compounds (oligomers up to C_{30} and C_{21}, respectively). Oligomer distributions for various temperatures are listed in Table I. Similar effects (i.e. decreasing polymer molecular weight with increasing temperature) have been observed in other Ziegler–Natta type polymerizations.[8] Although the shift toward lower molecular weight with increasing temperature can be partially attributed to the decrease in propene concentration, lower molecular weights are also expected on thermodynamic grounds.[9] Unfortunately, at temperatures where selectivity for dimerization for 2 exceeds 95% (i.e. at temperatures above 60 °C, Table I), the catalyst is inactive after about 15 productive cycles due to reaction of the cationic catalyst with the anion (vide infra).

Table I. Propene Oligomerization with 1 and 2 at Various Temperatures: Weight Fractions (%) As Determined by Gas Chromatography

	oligomers $(C_3H_6)_n$, n values						
T, °C	2	3	4	5	6	7	8
	Catalyst 1 (M = Zr)						
15	28	20	16	11	9	7	6
25	38	24	16	11	8	7	
35	51	25	13	7	3	1	
45	74	21	5				
55	80	15	12				
65	86	8	5				
	Catalyst 2 (M = Hf)						
15	46	27	16	9	2		
25	72	28					
35	82	18					
45	90	10					
55	93	7					
65	96	4					

Scheme I

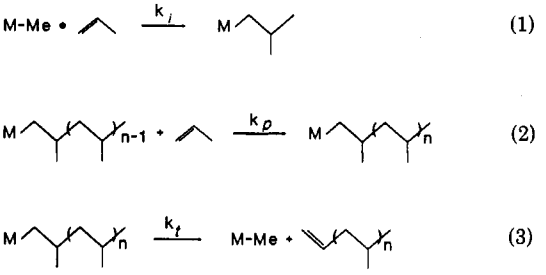

Effect of Temperature on Oligomerization. Kinetics. At 25 °C, over 97% of the products resulting from the catalytic oligomerization of propene with $[Cp^*_2MMe(THT)]^+[BPh_4]^-$ (1, M = Zr; 2, M = Hf) can be explained by the reactions shown in Scheme I.[6] For such a (homogeneous) oligomerization reaction with single initiation, propagation, and termination steps with k_i, k_p, and k_t remaining constant throughout the oligomerization and in which inactivation of the catalyst is negligible, the Flory–Schulz distribution is valid:[10]

$$m_P = P\alpha^P \ln^2 \alpha \qquad \text{(a)}$$

with m_P denoting the weight fraction of oligomer with degree of oligomerization P and α denoting the probability of the propagation step with[10a]

$$\frac{\alpha}{(1-\alpha)} = \frac{k_p}{k_t}[C_3H_6] \qquad \text{(b)}$$

Values for m_P can be determined from gas chromatographic analysis of the oligomerization reactions. According to (a), a plot of ln (m_P/P) versus P yields a straight line with slope ln α. With our oligomerization reactions two assumptions have to be made to allow the application of the Flory–Schulz theory. Inactivation of the catalyst should be slow relative to the insertion, propagation, and termination steps, and termination reactions other than β-Me elimination (e.g. β-H elimination) have to be negligible. At the temperature range studied (5–95 °C) oligomerization products due to β-H elimination accounted for less than 3% of the total propene consumption.

(8) Boor, J., Jr. *Ziegler-Natta Catalysts and Polymerizations*; Academic Press: New York, 1979; Chapter 18.

(9) Sawada, H. In *Thermodynamics of Polymerization*; O'Driscoll, K. F., Ed.; Marcel Dekker, Inc.: New York, 1976.

(10) (a) Henrici-Olivé, G.; Olivé, S. *Adv. Polym. Sci.* **1974**, *15*, 1. (b) Kissin, Y. V.; Beach, D. L. *J. Polym. Sci., Part A: Polym. Chem.* **1989**, *27*, 147.

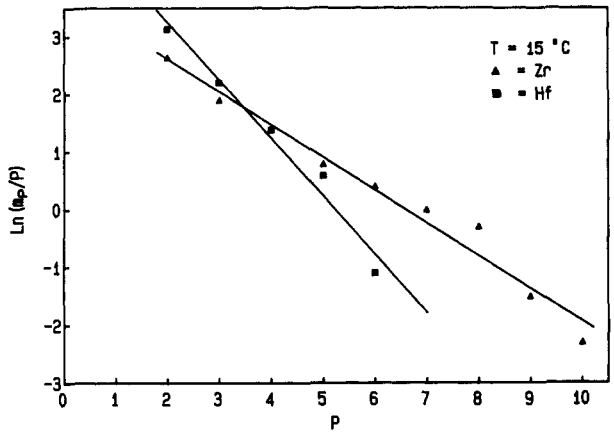

Figure 2. Plot of ln (m_P/P) vs P for oligomerization of propene at 15 °C with 1 and 2 as catalysts.

Table II. α Values and k_p/k_t Ratios for Propene Oligomerization with 1 and 2 as a Function of Temperature

	α		k_p/k_t[a]	
T, °C	1	2	1	2
5	0.96 (5)	0.77 (2)	36.2 (6)	20.9 (1.3)
15	0.85 (3)	0.59 (5)	25.2 (7)	15.1 (1.0)
25	0.63 (3)	0.39 (2)	17.3 (5)	11.2 (2)
35	0.41 (6)	0.22 (2)	11.4 (5)	8.3 (5)
45	0.26 (1)	0.11 (2)	9.5 (3)	6.1 (9)

[a] k_p = rate constant for propagation, k_t = rate constant for termination.

Table III. Values for $(\Delta H^{\ddagger}_p - \Delta H^{\ddagger}_t)$, $(\Delta S^{\ddagger}_p - \Delta S^{\ddagger}_t)$, and $(\Delta G^{\ddagger}_p - \Delta G^{\ddagger}_t)_{298K}$ for the Oligomerization of Propene with 1 and 2

compd	$(\Delta H^{\ddagger}_p - \Delta H^{\ddagger}_t)$, kcal·mol^{-1}	$(\Delta S^{\ddagger}_p - \Delta S^{\ddagger}_t)$, cal·mol^{-1}·K^{-1}	$(\Delta G^{\ddagger}_p - \Delta G^{\ddagger}_t)_{298K}$, kcal·mol^{-1}
1	−7.5 (1)	−18.7 (5)	−1.9 (3)
2	−5.5 (2)	−13.8 (6)	−1.4 (4)

Therefore it is reasonable to neglect this termination step in a first approximation. At temperatures above 45 °C inactivation is no longer negligible, leading to deviations from the Flory–Schulz distribution. Good correlations were obtained over the temperature range from 5 to 45 °C (Figure 2), indicating that for these temperatures our assumptions were valid. An important conclusion that can be derived from the Flory–Schulz behavior is that $[Cp^*_2MMe(THT)]^+[BPh_4]^-$ (M = Zr, Hf) act as true single-sited catalysts.[11] Table II contains the α values together with the corresponding k_p/k_t ratios for propene oligomerization at five different temperatures for both catalytic systems. The k_p/k_t ratios strongly depend on the reaction temperature and decrease with increasing temperature. The ratios are related to the differences in entropy and to the enthalpy of activation for propagation and β-methyl elimination via

$$k_p/k_t = \exp\{-[(\Delta H^{\ddagger}_p - \Delta H^{\ddagger}_t)/RT - (\Delta S^{\ddagger}_p - \Delta S^{\ddagger}_t)/R]\} \quad (c)$$

Plots of ln (k_p/k_t) versus $1/T$ for 1 and 2 yield straight lines with slope $-(\Delta H^{\ddagger}_p - \Delta H^{\ddagger}_t)/R$ and $(\Delta S^{\ddagger}_p - \Delta S^{\ddagger}_t)/R$ as the y intercept. These plots are shown in Figure 3, while the values of $(\Delta H^{\ddagger}_p - \Delta H^{\ddagger}_t)$, $(\Delta S^{\ddagger}_p - \Delta S^{\ddagger}_t)$, and $(\Delta G^{\ddagger}_p - \Delta G^{\ddagger}_t)_{298K}$ are listed in Table III. Although the experimental results indicate that $\Delta\Delta G^{\ddagger}_{298K}$ for 2 is smaller than for 1, the calculated values do not permit a definite conclusion due to the experimental error.

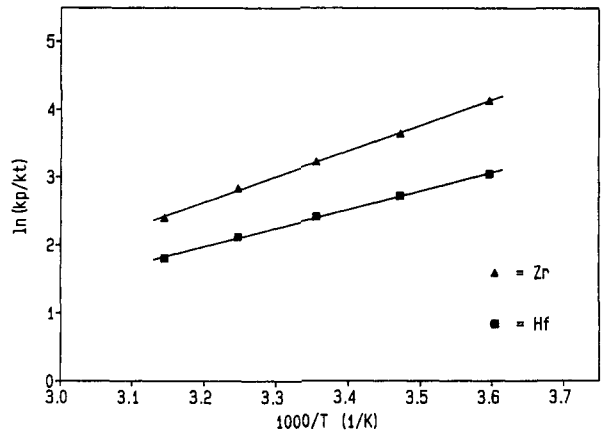

Figure 3. Plot of ln (k_p/k_t) for 1 and 2 against the temperature.

Table IV. Selected Bond Distances (Å) and Angles (deg) for $[Cp^*_2ZrMe(THT)]^+[BPh_4]^-$ (1) and $[Cp^*_2HfMe(THT)]^+[BPh_4]^-$ (2)[a]

	Data for 1		
	Bond Distances		
Zr1–S1	2.730 (4)	Zr1–C14	2.519 (9)
Zr1–C25	2.242 (8)	Zr1–C15	2.533 (9)
Zr1–C1	2.52 (1)	Zr1–C1x	2.228 (4)
Zr1–C2	2.508 (8)	Zr1–C2x	2.238 (4)
Zr1–C3	2.54 (1)	S1–C21	1.81 (1)
Zr1–C4	2.542 (9)	S1–C24	1.83 (1)
Zr1–C5	2.562 (9)	C21–C22	1.50 (2)
Zr1–C11	2.564 (9)	C22–C33	1.50 (2)
Zr1–C12	2.556 (9)	C23–C24	1.53 (1)
Zr1–C13	2.53 (1)		
	Bond Angles		
Si–Zr1–C25	81.5 (2)	C25–Zr1–C1x	104.5 (3)
C1x–Zr1–C2x	138.2 (3)	C25–Zr1–C2x	104.0 (3)
S1–Zr1–C1x	113.5 (3)	C21–S1–C24	95.0 (5)
	Data for 2		
	Bond Distances		
Hf1–S1	2.626 (4)	Hf1–C14	2.47 (1)
Hf1–C25	2.233 (9)	Hf1–C15	2.49 (1)
Hf1–C1	2.63 (1)	Hf1–C1x	2.344 (4)
Hf1–C2	2.59 (1)	Hf1–C2x	2.147 (8)
Hf1–C3	2.66 (1)	S1–C21	1.87 (2)
Hf1–C4	2.67 (1)	S1–C24	1.83 (2)
Hf1–C5	2.65 (1)	C21–C22	1.52 (2)
Hf1–C11	2.48 (1)	C22–C33	1.53 (2)
Hf1–C12	2.44 (1)	C23–C24	1.54 (3)
Hf1–C13	2.44 (1)		
	Bond Angles		
S1–Hf1–C25	83.2 (3)	C25–Hf1–C1x	102.6 (4)
C1x–Hf1–C2x	135.6 (4)	C25–Hf1–C2x	106.8 (4)
S1–Hf1–C1x	112.4 (4)	C21–S1–C24	94.1 (7)
S1–Hf1–C2x	103.7 (4)		

[a] Cnx denotes Cp* ring centroid; C1x = C1--C5, C2x = C11--C15.

Solid-State Structures of $[Cp^*_2ZrMe(THT)]^+[BPh_4]^-$ and $[Cp^*_2HfMe(THT)]^+[BPh_4]^-$. The solid-state structures of 1 and 2 were determined by single-crystal X-ray diffraction and consist of discrete $[Cp^*_2MMe(THT)]^+$ and $[BPh_4]^-$ ions of normal geometry.[12] Both structures are very similar; therefore only an ORTEP view of the cation of 1 is given (Figure 4). Selected bond lengths and angles for both compounds are listed in Table IV (Zr, Hf), and atomic coordinates are listed in Tables V (Zr) and VI (Hf). The cations adopt the normal bent metallocene structure, with the CH_3 and THT ligands

(11) Peebles, L. H., Jr. *Polym. Rev.* **1971**, *18*, 1.

(12) (a) Glidewell, C.; Holden, H. D. *Acta Crystallogr., Sect. B* **1982**, *38*, 669. (b) Watkins, M. I.; Ip, W. M.; Olah, G. A.; Bau, R. *J. Am. Chem. Soc.* **1982**, *104*, 2365.

Table V. Final Fractional Coordinates and Equivalent Isotropic Thermal Parameters for $[Cp^*_2ZrMe(THT)]^+[BPh_4]^-$

atom	x/z	y/b	z/c	U_{eq},[a] Å^2
Zr(1)	0.10602 (2)	0.09370 (6)	1.00035 (–)	0.0177 (2)
S(1)	0.15850 (11)	0.2028 (3)	0.8420 (3)	0.0402 (11)
C(1)	0.1481 (3)	0.1944 (10)	1.1622 (11)	0.022 (4)
C(2)	0.1063 (3)	0.2394 (7)	1.1645 (7)	0.018 (3)
C(3)	0.0784 (3)	0.1543 (9)	1.2061 (9)	0.020 (3)
C(4)	0.1021 (3)	0.0531 (7)	1.2253 (8)	0.022 (3)
C(5)	0.1466 (3)	0.0802 (8)	1.2006 (8)	0.024 (3)
C(6)	0.1880 (3)	0.2658 (8)	1.1478 (9)	0.035 (4)
C(7)	0.0935 (2)	0.3581 (7)	1.1337 (9)	0.026 (3)
C(8)	0.0348 (3)	0.1754 (9)	1.2534 (9)	0.040 (4)
C(9)	0.0879 (3)	–0.0532 (8)	1.2845 (9)	0.039 (4)
C(10)	0.1837 (3)	0.0044 (8)	1.2283 (9)	0.038 (4)
C(11)	0.0622 (3)	–0.0473 (7)	0.8759 (9)	0.023 (3)
C(12)[b]	0.0748 (3)	0.0369 (8)	0.7961 (9)	0.018 (2)
C(13)	0.0560 (3)	0.1398 (8)	0.8279 (9)	0.023 (4)
C(14)	0.0297 (3)	0.1186 (7)	0.9334 (9)	0.026 (3)
C(15)	0.0339 (3)	0.0040 (8)	0.9612 (7)	0.019 (3)
C(16)	0.0716 (3)	–0.1701 (7)	0.8640 (9)	0.029 (4)
C(17)	0.1014 (3)	0.0174 (10)	0.6823 (8)	0.044 (4)
C(18)	0.0559 (4)	0.2519 (8)	0.7628 (10)	0.050 (5)
C(19)	–0.0039 (3)	0.2004 (8)	0.9774 (11)	0.050 (5)
C(20)	0.0087 (3)	–0.0622 (8)	1.0517 (8)	0.041 (4)
C(21)	0.2147 (3)	0.1695 (9)	0.8573 (10)	0.042 (4)
C(22)	0.2378 (3)	0.2703 (3)	0.8064 (10)	0.056 (5)
C(23)	0.2146 (3)	0.3733 (9)	0.8509 (11)	0.049 (5)
C(24)	0.1664 (3)	0.3556 (9)	0.8407 (11)	0.056 (5)
C(25)	0.1532 (2)	–0.0456 (7)	0.9689 (7)	0.021 (3)
C(26)	0.0912 (3)	0.5329 (7)	0.5263 (10)	0.025 (4)
C(27)	0.0798 (3)	0.5709 (7)	0.6436 (9)	0.027 (3)
C(28)	0.0402 (3)	0.5498 (8)	0.6968 (10)	0.036 (4)
C(29)	0.0097 (3)	0.4904 (8)	0.6344 (10)	0.036 (4)
C(30)	0.0181 (3)	0.4534 (8)	0.5197 (12)	0.037 (4)
C(31)	0.0581 (3)	0.4754 (8)	0.4691 (9)	0.035 (4)
C(32)	0.1648 (3)	0.4268 (7)	0.4817 (10)	0.022 (4)
C(33)	0.2101 (3)	0.4217 (7)	0.4850 (11)	0.024 (3)
C(34)	0.2326 (3)	0.3223 (7)	0.4836 (10)	0.025 (3)
C(35)	0.2107 (3)	0.2198 (8)	0.4817 (10)	0.033 (4)
C(36)	0.1666 (3)	0.2203 (8)	0.4792 (10)	0.030 (4)
C(37)	0.1454 (3)	0.3222 (7)	0.4777 (8)	0.021 (3)
C(38)	0.1375 (3)	0.5821 (8)	0.3232 (8)	0.024 (3)
C(39)	0.1017 (3)	0.6305 (7)	0.2684 (8)	0.030 (4)
C(40)	0.1018 (4)	0.6594 (7)	0.1440 (8)	0.031 (4)
C(41)	0.1378 (3)	0.6428 (7)	0.0754 (9)	0.031 (4)
C(42)	0.1735 (3)	0.5946 (8)	0.1267 (8)	0.033 (4)
C(43)	0.1729 (3)	0.5645 (8)	0.2501 (9)	0.030 (4)
C(44)	0.1642 (3)	0.6499 (7)	0.5401 (7)	0.017 (3)
C(45)	0.1824 (3)	0.6331 (8)	0.6552 (9)	0.030 (4)
C(46)	0.2020 (3)	0.7191 (8)	0.7196 (9)	0.032 (4)
C(47)	0.2037 (3)	0.8256 (9)	0.6763 (10)	0.036 (4)
C(48)	0.1861 (3)	0.8467 (8)	0.5618 (9)	0.033 (4)
C(49)	0.1670 (2)	0.7601 (7)	0.4992 (14)	0.028 (3)
B(1)	0.1388 (4)	0.5473 (9)	0.4704 (9)	0.024 (4)

[a] $U_{eq} = {}^1/_3\sum_i\sum_j U_{ij}a_i^*a_j^*\mathbf{a}_i\cdot\mathbf{a}_j$. [b] Nonpositive definite temperature factors returned to isotropic thermal displacement factors.

Table VI. Final Fractional Coordinates and Equivalent Isotropic Thermal Parameters for $[Cp^*_2HfMe(THT)]^+[BPh_4]^-$

atom	x/a	y/b	z/c	U_{eq},[a] Å^2
Hf(1)	0.10666 (1)	0.08981 (3)	1.00035 (–)	0.0155 (1)
S(1)	0.15892 (16)	0.1956 (5)	0.8532 (4)	0.0300 (16)
C(1)[b]	0.1474 (6)	0.1975 (16)	1.1729 (16)	0.019 (4)
C(2)	0.1059 (5)	0.2374 (10)	1.1724 (12)	0.025 (4)
C(3)	0.0792 (6)	0.1540 (13)	1.2168 (15)	0.027 (6)
C(4)[b]	0.1036 (5)	0.0508 (11)	1.2376 (12)	0.020 (3)
C(5)	0.1470 (4)	0.0782 (12)	1.2095 (11)	0.020 (4)
C(6)	0.1873 (5)	0.2656 (15)	1.1604 (15)	0.041 (6)
C(7)	0.0929 (6)	0.3555 (12)	1.1421 (15)	0.043 (7)
C(8)	0.0353 (5)	0.1730 (14)	1.2677 (15)	0.038 (6)
C(9)	0.0886 (6)	–0.0523 (12)	1.2999 (15)	0.038 (6)
C(10)	0.1845 (6)	0.0022 (14)	1.2407 (15)	0.039 (6)
C(11)	0.0627 (5)	–0.0480 (12)	0.8869 (13)	0.024 (4)
C(12)	0.0768 (5)	0.0353 (12)	0.8051 (12)	0.018 (4)
C(13)	0.0582 (5)	0.1383 (13)	0.8359 (15)	0.025 (5)
C(14)	0.0313 (5)	0.1197 (10)	0.9438 (13)	0.020 (4)
C(15)	0.0346 (5)	0.0047 (12)	0.9723 (12)	0.028 (6)
C(16)	0.0719 (6)	–0.1708 (12)	0.8781 (15)	0.035 (6)
C(17)[b]	0.1023 (5)	0.0162 (14)	0.6940 (15)	0.035 (4)
C(18)	0.0573 (7)	0.2520 (13)	0.7780 (18)	0.056 (7)
C(19)	–0.0026 (5)	0.2005 (12)	1.001 (3)	0.083 (8)
C(20)	0.0088 (6)	–0.0589 (13)	1.0638 (14)	0.041 (6)
C(21)	0.2166 (5)	0.1612 (14)	0.8760 (17)	0.039 (6)
C(22)	0.2393 (6)	0.2625 (15)	0.8221 (16)	0.049 (7)
C(23)	0.2157 (6)	0.3679 (15)	0.8637 (18)	0.050 (7)
C(24)	0.1674 (6)	0.3486 (13)	0.8523 (19)	0.047 (7)
C(25)[b]	0.1534 (3)	–0.0510 (8)	0.9784 (9)	0.008 (3)
C(26)	0.0894 (6)	0.5283 (12)	0.5387 (13)	0.034 (5)
C(27)	0.0798 (5)	0.5696 (11)	0.6552 (15)	0.032 (5)
C(28)	0.0402 (6)	0.5484 (12)	0.7090 (16)	0.043 (6)
C(29)	0.0096 (5)	0.4879 (12)	0.6520 (16)	0.036 (6)
C(30)	0.0188 (6)	0.4502 (12)	0.5333 (14)	0.041 (7)
C(31)	0.0573 (5)	0.4704 (11)	0.4781 (10)	0.020 (5)
C(32)	0.1644 (4)	0.4255 (10)	0.502 (3)	0.028 (4)
C(33)	0.2092 (4)	0.4216 (10)	0.509 (3)	0.031 (4)
C(34)	0.2329 (4)	0.3202 (10)	0.496 (2)	0.021 (4)
C(35)	0.2108 (5)	0.2170 (11)	0.493 (3)	0.031 (5)
C(36)[b]	0.1667 (4)	0.2175 (11)	0.4858 (16)	0.030 (4)
C(37)	0.1449 (4)	0.3195 (11)	0.494 (3)	0.032 (5)
C(38)	0.1379 (5)	0.5794 (12)	0.3346 (13)	0.026 (4)
C(39)	0.1018 (5)	0.6300 (11)	0.2807 (13)	0.026 (4)
C(40)	0.1012 (5)	0.6598 (12)	0.1590 (13)	0.031 (5)
C(41)	0.1384 (6)	0.6385 (12)	0.0855 (14)	0.044 (6)
C(42)	0.1729 (6)	0.5936 (14)	0.1400 (13)	0.038 (5)
C(43)	0.1734 (5)	0.5642 (11)	0.2598 (13)	0.023 (5)
C(44)	0.1639 (5)	0.6474 (13)	0.5555 (13)	0.029 (5)
C(45)	0.1808 (5)	0.6296 (13)	0.6700 (14)	0.032 (5)
C(46)	0.2007 (5)	0.7166 (13)	0.7383 (15)	0.033 (5)
C(47)	0.2036 (5)	0.8233 (13)	0.6867 (14)	0.031 (5)
C(48)	0.1873 (5)	0.8454 (13)	0.5773 (14)	0.035 (5)
C(49)	0.1679 (4)	0.7587 (10)	0.5182 (18)	0.019 (4)
B(1)	0.1371 (5)	0.5494 (14)	0.497 (4)	0.049 (7)

[a] $U_{eq} = {}^1/_3\sum_i\sum_j U_{ij}a_i^*a_j^*\mathbf{a}_i\cdot\mathbf{a}_j$. [b] Nonpositive definite temperature factors returned to isotropic thermal displacement factors.

arranged in the plane between the two Cp* ligands. The M–C25 distances of 2.242 (8) Å in **1** and 2.233 (9) Å in **2** are at the short side of the range of values reported for M–CH_3 (M = Zr, Hf) distances (average 2.292 (49) Å (M = Zr), 2.275 (49) Å (M = Hf)[13]) but agree well with Zr–CH_3 distances in other cationic zirconium complexes (cf. 2.240 (4) Å in $(C_5Me_4Et)_2ZrMe(C_2B_9H_{12})$[3f] and 2.256 (10) Å in $[Cp_2ZrMe(THT)]^+[BPh_4]^-$[3b]).

On the basis of the strong similarity between zirconium and hafnium, both with respect to size and chemical properties, one expects compounds with almost identical structures. At first view this is the case, but there are a few differences, even when one realizes that the accuracy of the determination for **2** is not very high. Whereas the zirconium atom is placed symmetrically between the two cyclopentadienyl ligands (Zr–Cp*1 = 2.23 (3), Zr–Cp*2 = 2.24 (5) Å, Cp*1 = plane through C1--C5, Cp*2 = plane through C11--C15), the distances of the hafnium atom to the rings are different: Hf–Cp*1 = 2.34 (4) vs Hf–Cp*2 = 2.14 (8) Å. The other difference is the M–S distance in **1** and **2**. The Zr1–S1 distance (2.730 (4) Å) is typical for early-transition-metal sulfur bonds.[3l,14-16] The Hf1–S1 distance (2.626 (4) Å) is significantly shorter. These are the only clear differences between both structures. The bond lengths and angles within the ligands are equal and

(13) Orpen, A. G.; Brammer, L.; Allen, F. H.; Kennard, O.; Watson, D. G.; Taylor, R. *J. Chem. Soc., Dalton Trans.* **1989**, S1.

(14) Campiolini, M.; Mealli, C.; Nardi, N. *J. Chem. Soc., Dalton Trans.* **1980**, 376.

(15) Gambarotta, S.; Chiesi-Villa, A.; Guastini, C. *Inorg. Chem.* **1988**, *27*, 99.

(16) Templeton, J. L.; Dorman, W. C.; Clardy, J. C.; McCarley, R. E. *Inorg. Chem.* **1978**, *17*, 1263.

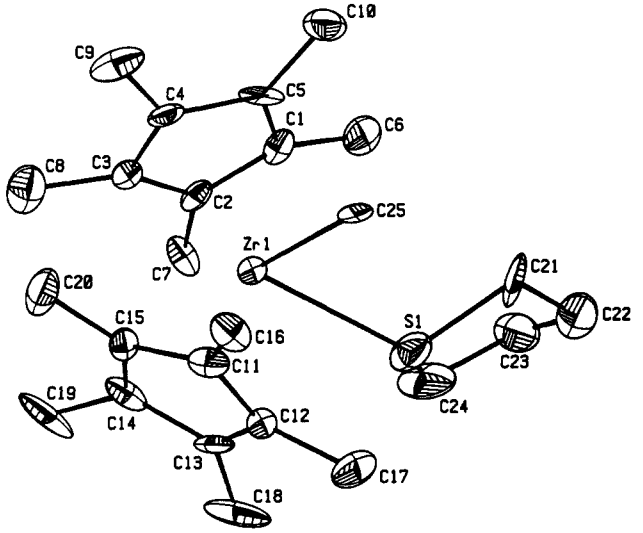

Figure 4. Perspective ORTEP view with adopted numbering scheme of $[Cp^*_2ZrMe(THT)]^+$ (hydrogen atoms omitted for clarity). All atoms are represented by their thermal vibrational ellipsoids drawn to encompass 50% of the electron density.

so are the M–C25 bonds. The coordinated THT ligands are oriented out of the C25–M–S1 plane (dihedral angle between the C25–M–S1 plane and the THT C21–S1–C24 plane 44.2 (6)° in 1 and 44.4 (9)° in 2; angle between the M–S vector and the THT C21–S1–C24 plane 43.3 (5)° in 1 and 43.4 (8)° in 2). It is tempting to consider the short Hf–S bond as the result of a considerable interaction of the lone electron pair on sulfur and the Lewis acidic metal center, which forces the metal into an usual position between the cyclopentadienyl ligands. That this is not observed in the zirconium derivative 1 could indicate a substantial difference in Lewis acidity between the two metals: hafnium appears to be softer than zirconium. It would be necessary to verify this and compare with structural data of related compounds. Unfortunately, structure determinations of hafnium compounds are very scarce and the information needed is not available. The short Hf–S distance in 2 leads to a distortion of the Cp^*_2Hf fragment: the Hf1–C1x distance (2.343 (6) Å) is the longest Hf–centroid distance observed so far, whereas the Hf–C2x distance (2.147 (6) Å) is at the low end of the range normally observed.[17] The C–C bond lengths and angles within the Cp* ligands are normal geometry. An analogous asymmetric bonding of Cp* ligands was observed in the isoelectronic complex $Cp^*_2YMe{\cdot}THF$,[18] but no explanation for the inequivalent distances of Y to the Cp* planes was given there. The Zr–centroid distances are equal and lie in the range normally observed for other cationic and neutral permethylzirconocene complexes.[3f,19] Surprisingly, the short Hf–S distance and the asymmetric position of the hafnium atom between the Cp* ligands do not lead to strong steric repulsions in the molecule. When the intramolecular contacts are inspected, it appears that both 1 and 2 have short but comparable contacts at the same positions, viz. where the Cp* rings touch (C8 and C16, C8 and C19) and between the THT ligand and the front of the Cp^*_2M wedge (C21–C6).

β-Me Elimination versus β-H Elimination. The dominant termination by β-Me elimination in the oligomerization of propene with $[Cp^*_2MMe(THT)]^+[BPh_4]^-$ (M = Zr, Hf)[6] is surprising since the hydride complexes $[Cp^*_2MH]^+$ resulting from β-H elimination are predicted to be ca. 10 kcal.mol^{-1} more stable than the methyl complexes $[Cp^*_2MMe]^+$.[20] Therefore the tendency of $[Cp^*_2M–CH_2–C(H)(CH_3)–R]^+$ to undergo β-methyl elimination has to be kinetic in origin. A possible explanation might be that in complexes with bulky Cp* groups an orientation of the β-Me substituent of the growing chain in the equatorial plane of the Cp^*_2M wedge that contains the Zr LUMO[21] (structure A) is more favorable than an

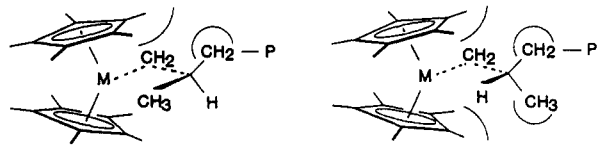

A B

orientation with the β-Me group pointing toward one of the Cp* rings (structure B) due to steric interactions. In this way, transfer of the methyl group from a growing oligomer chain to the metal is kinetically favored over β-H transfer. Similar steric arguments were used by Bercaw et al. to explain the presence of an agostic interaction in $Cp^*_2ScCH_2CH_3$ and the absence of such an interaction in $Cp^*_2ScCH_2CH_2CH_3$.[2g] Minimization of the potential energy of $[Cp^*_2ZrCH_2CH(CH_3)CH_2CH(CH_3)_2]^+$ (the compound that produces 4-methyl-1-pentene upon β-methyl elimination) with the ALCHEMY II softward package[22] indeed suggests that conformation A is about 4 kcal.mol^{-1} more stable than B. The main reason for the difference appears to be the close contact of the β-Me group with the Cp* methyl groups in conformation B, which is absent in conformation A.[23] If the calculated energy difference is real, then, as a result of the lower energy of A, over 99% of the molecules will be in this conformation, as predicted by the Boltzmann distribution (T = 298 K). This percentage is reflected in the distribution of oligomeric products arising from the two different termination steps (β-Me elimination: 97%; β-H elimination: 3%). Therefore the activation energy for β-H transfer starting from B has to be comparable to the activation energy for β-Me transfer starting from A. The propensity for β-Me transfer then is due to differences in ground-state energy of the two conformations.

(17) (a) Van Asselt, A.; Santarsiero, B. D.; Bercaw, J. E. *J. Am. Chem. Soc.* **1986**, *108*, 8291. (b) Bulls, A. R.; Schaefer, W. P.; Serfas, M.; Bercaw, J. E. *Organometallics* **1987**, *6*, 1219. (c) Hillhouse, G. L.; Bulls, A. R.; Santarsiero, B. D.; Bercaw, J. E. *Organometallics* **1988**, *7*, 1309.

(18) den Haan, K. H.; de Boer, J. L.; Teuben, J. H.; Smeets, W. J. J.; Spek, A. L. *J. Organomet. Chem.* **1987**, *327*, 31.

(19) (a) Wolczanski, P. T.; Threlkel, R. S.; Bercaw, J. E. *J. Am. Chem. Soc.* **1979**, *101*, 218. (b) Moore, E. J.; Straus, D. A.; Armentrout, J.; Santarsiero, B. D.; Grubbs, R. H.; Bercaw, J. E. *J. A. Chem. Soc.* **1983**, *105*, 2068. (c) Barger, P. T.; Santarsiero, B. D.; Armentrout, J.; Bercaw, J. E. *J. Am. Chem. Soc.* **1984**, *106*, 5178. (d) Schock, L. E.; Brock, C. P.; Marks, T. J. *Organometallics* **1987**, *6*, 232. (e) Cardin, D. J.; Lappert, M. F.; Raston, C. L. *Chemistry of Organo Zirconium and -Hafnium Compounds*; Ellis Horwood Ltd.: West Sussex, U.K., 1986; Chapter 4.

(20) Schock, L. E.; Marks, T. J. *J. Am. Chem. Soc.* **1988**, *110*, 7701.

(21) Lauher, J. W.; Hoffmann, R. *J. Am. Chem. Soc.* **1976**, *98*, 1729.

(22) ALCHEMY II; Tripos Associates, Inc., St. Louis; MO 1987. For reviews of the program see: (a) Newkome, G. R. *J. Am. Chem. Soc.* **1988**, *110*, 325. (b) Sadek, M.; Munro, S. *J. Comput.-Aided Mol. Design* **1988**, *2*, 81.

(23) (a) To test the molecular modeling studies, an attempt was made to synthesize $[Cp^*_2HfCH_2CHMe_2]^+$ by protonation of $Cp^*_2HfH(CH_2CHMe_2)$.[23b] If a conformation with one of the β-methyl groups in the equatorial plane would be lower in energy than a conformation with the β-hydrogen atom in the equatorial plane, the Cp* ligands would be magnetically inequivalent, provided that rotation around the M–C carbon σ bond interconverting the two conformations would be slow on the NMR time scale. Unfortunately, preliminary results (NMR analysis, THF-d_8, room temperature) indicate that the cationic Hf–isobutyl complex is not produced but instead isobutane is extruded with the formation of the cationic hydride $[Cp^*_2HfH(THF\text{-}d_8)]^+[BPh_4]^-$. (b) Roddick, D. M.; Fryzuk, M. D.; Seidler, P. F.; Hillhouse, G. L.; Bercaw, J. E. *Organometallics* **1985**, *4*, 97.

Catalyst Inactivation. The catalysts are slowly inactivated during the oligomerization. For example at room temperature turnover numbers are 150 and 370 mol of C_3H_6/mol of M for **1** and **2**, respectively. To identify the inactivation process, the following experiment was carried out. Propene was oligomerized at 25 °C with either **1** or **2** as the catalyst. After monomer uptake had ceased, the volatiles were pumped off and D_2O was added. Gas (1 equiv) was liberated (Toepler pump) that was shown by GC and MS to consist of a mixture of propene-d_1 and isobutene-d_1 (M = Zr, C_3H_5D/C_4H_7D = 0.3/0.7; M = Hf, C_3H_5D/C_4H_7D = 0.4/0.6). These results indicate that both catalysts **1** and **2** are inactivated by formation of allyl and 2-methallyl complexes, respectively, presumably by allylic C-H activation. The same type of inactivation has been observed in the reaction of propene with lanthanide complexes Cp^*_2LuMe,[2b] $[\{Me_2Si(C_5Me_4)_2\}LuH]_2$,[24] and $[Cp^*_2LnH]_2$ (Ln = La,[2d] Nd,[2d] Sm[25]). This emphasizes the close resemblance of cationic group 4 compounds and the isoelectronic lanthanide complexes.

Especially, the formation of the methallyl complexes is noteworthy, since isobutene is only formed in very small amounts by β-hydrogen elimination during the oligomerization of propene.[6] Apparently, isobutene is a very efficient trapping agent for $[Cp^*_2MR]^+$ (M = Zr, Hf). To test this hypothesis, a solution of **1** was exposed to isobutene (5-fold molar excess). Reaction with D_2O after the excess olefin had been pumped off liberated 1 equiv of gas that was identified as $CH_2{=}C(CH_2D)(CH_3)$ by NMR spectroscopy. These results strongly suggest that $[Cp^*_2MR]^+$ (M = Zr, Hf) indeed reacts with isobutene to give a methallyl complex. Vinylic C—H activation producing a complex of the type $[Cp^*_2Zr{-}CH{=}CMe_2]^+$, as has been observed in the reaction of $Cp^*_2ScCH_3$ with isobutene,[2e] can be excluded since $[Cp^*_2Zr{-}CH{=}CMe_2]^+$ would produce $CDH{=}CMe_2$ upon reaction with D_2O.

Addition of hydrogen (10-fold molar excess) to the oligomerization reaction mixture after olefin uptake had ceased restored catalytic activity. Hydrogenolysis of the M–allyl bond results in the formation of a metal hydride that can reinitiate the oligomerization. The resulting hydrogen however competes with the insertion reaction by hydrogenolyzing the M–C σ bond at the growing end of the oligomer chain, giving a shift toward lower oligomer molecular weights and oligomerization products with saturated end groups.

At higher temperatures a different inactivation occurs. After an oligomerization had been carried out at 55 °C with either **1** or **2** as the catalyst, the mixture was quenched with D_2O after propene uptake had ceased and all volatiles had been pumped off. No propene, isobutene, or other gaseous products were observed. A possible explanation might be that at these tempertaures the catalysts decompose by metalation of one of the phenyl rings of the anion with extrusion of alkane to give zwitterionic complexes of the type $Cp^*_2M^+$-*m*-C_6H_4–BPh_3^-,[3f] as recently described by Turner et al. (eq d). Analogous metalation of aromatic

$$[Cp^*_2M{-}R]^+[BPh_4]^- \rightarrow Cp^*_2M^+\text{-}m\text{-}C_6H_4\text{-}BPh_3^- + RH \quad \text{(d)}$$

R = CH_3 or growing oligomer chain

M = Zr, Hf

rings has been observed in the reaction of Cp^*_2LuMe and Cp^*_2ScMe with benzene to give $Cp^*_2LuC_6H_5$ and $Cp^*_2ScC_6H_5$, respectively, and methane.[2c,e] Clear proof in favor of phenyl metalation was obtained by thermolyzing $[Cp^*_2HfMe(THT)]^+[B(C_6D_5)_4]^-$ in *N*,*N*-dimethylaniline ($PhNMe_2$) at 55 °C. Gas (1 equiv) (Toepler pump) was liberated that was identified as CH_3D by MS. The intermediacy of a fulvene complex $[Cp^*(\eta^5,\eta^1\text{-}C_5Me_4CH_2)Hf]^+$ or proton abstraction from the solvent in the thermolysis can be ruled out since this would in both cases require the liberation of CH_4 instead of CH_3D. Inactivation by formation of zwitterionic complexes only occurs at higher temperatures. Solutions of $[Cp^*_2MMe(THT)]^+[BPh_4]^-$ (M = Zr, Hf) in $PhNMe_2$ are stable at room temperature for at least 24 h.[6]

Conclusions

The complexes $[Cp^*_2MMe(THT)]^+[BPh_4]^-$ (M = Zr, Hf) are active catalysts for the oligomerization of propene. The product distribution strongly depends on the reaction temperature giving decreasing molecular weights with increasing temperature. The oligomer molecular weights are satisfactorily described by the Flory–Schulz theory over the temperature range 5–45 °C. This allows the calculation of the rate ratio for propagation and termination and to quantify the differences in activation parameters.

The dominant termination step is β-Me transfer from the growing oligomer chain to the metal. Molecular modeling studies on the basis of the molecular structures of the active catalysts suggest that the preference for this termination is due to a lower ground-state energy for the conformation with the β-Me substituent on the growing oligomer chain in the equatorial plane in the Cp^*_2M wedge.

At room temperature the catalysts are slowly inactivated by allylic C–H activation of propene or isobutene (formed by a minor β-H-transfer mechanism) to give (meth)allyl complexes. At elevated temperatures (>50 °C) catalytically inactive zwitterionic complexes $Cp^*_2M^+$-*m*-C_6H_4–BPh_3^- are formed through aromatic C–H activation. Reactivation of the inactive (meth)allyl complexes can be achieved by addition of hydrogen to the oligomerization mixtures.

Experimental Section

General Considerations. All experiments were performed under nitrogen using standard Schlenk, vacuum line, and drybox (Braun MB200) techniques. $[Cp^*_2ZrMe(THT)]^+[BPh_4]^-$ (**1**) and $[Cp^*_2HfMe(THT)]^+[BPh_4]^-$ (**2**) were prepared according to literature procedures.[6] $NaB(C_6D_5)_4$ was synthesized analogously to $NaB(C_6H_5)_4$.[26] $PhNMe_2$ and THT were distilled from potassium. Polymerization grade propene was supplied by DSM and used without further purification. Isobutene (CP) was purchased from Union Carbide and used as received. GC analyses were performed on a Packard/Becker 428 chromatograph using a CP Sil 5CB capillary column or on a Hewlett-Packard 5890 A using a Hewlett-Packard OV-101 column. Quantification of the GC data was accomplished by calculating response factors from analysis of an external standard solution (4-methyl-1-pentene and 4,6-dimethyl-1-heptene). For the higher oligomers standard compounds were not available and their response factors were assumed to be linearly related to their carbon number and were scaled accordingly. Mass spectra were recorded on an AEI MS-902 instrument at 15 eV. NMR spectra were recorded on a Varian VXR-300 or Bruker WH-90-DS spectrometer and referenced to residual solvent protons (^1H NMR δ THF-d_8 = 3.57 ppm, δ C_6D_6 = 7.15, δ acetone-d_6 = 2.05; ^{13}C NMR δ THF-d_8 = 25.5 ppm). IR spectra were recorded on a Mattson-4020 Galaxy FT-IR spectrophotometer using Nujol mulls between KBr disks. Reaction temperatures were maintained by using a Techne Tempette

(24) Jeske, G.; Schock, L. E.; Swepston, P. N.; Schumann, H.; Marks, T. J. *J. Am. Chem. Soc.* **1985**, *107*, 8103.
(25) Nolan, S. P.; Stern, D.; Marks, T. J. *J. Am. Chem. Soc.* **1989**, *111*, 7844.
(26) Holzapfel, H.; Richter, C. *J. Prakt. Chem.* **1964**, *26* (4), 15.

TE-8D thermostated water bath and were observed to be constant to within ±0.1 °C.

General Remarks for Oligomerization Reactions. All oligomerization reactions were carried out with 50 mL of 4.0 mM solutions of 1 or 2 in $PhNMe_2$ at 1 atm of olefin pressure. Olefin uptake profiles were monitored using a Brooks 5850 TR mass flow meter on the gas feed line and recorded for analysis. Reactions were quenched with H_2O (D_2O) after monomer uptake had ceased. Propene concentrations at various temperatures were determined from experiments in which 50 mL of $PhNMe_2$ was saturated with propene under oligomerization conditions but in the absence of catalyst.

Reaction of 1 with Isobutene. A solution of 162 mg (0.21 mmol) of 1 in 10 mL of $PhNMe_2$ was exposed to 5 equiv isobutene on a vacuum line. After 1 h, excess of olefin was pumped off and 0.2 mL of D_2O (excess) added by vacuum transfer. Volatiles (0.20 mmol, 0.95 equiv) were collected by Toepler pump and analyzed (NMR spectroscopy). ^1H NMR (C_6D_6): δ 4.74 (sextet, $^4J_{HH}$ = 1.1 Hz, 2 H, CH_2=), 1.59 (t, $^4J_{HH}$ = 1.1 Hz, 5 H, =C(CH_3)(CH_2D)).

$[HNEt_3]^+[B(C_6D_5)_4]^-$. A suspension of 1.25 mL (9.0 mmol) NEt_3 in 25 mL of water was acidified with concentrated hydrochloric acid to pH = 1. The resulting solution was then added to a stirred solution of 3.00 g (8.3 mmol) $NaB(C_6D_5)_4$ in 100 mL of water, causing the precipitation of $[HNEt_3]^+[B(C_6D_5)_4]^-$. The ammonium salt was filtered off, washed thoroughly with water, dried, and crystallized from acetone to afford 2.11 g (4.8 mmol, 59%) of colorless crystals. The product was shown by NMR spectroscopy to be >95% deuterated. ^1H NMR (acetone-d_6): δ 3.32 (q, $^3J_{HH}$ = 7.3 Hz, 6 H, N-CH_2), 1.32 (t, $^3J_{HH}$ = 7.3 Hz, 9 H, -CH_3), NH not found (-10 to +30 ppm).

$[Cp^*_2HfMe(THT)]^+[B(C_6D_5)_4]^-$. A mixture of 1.114 g (2.33 mmol) $Cp^*_2HfMe_2$[22] and 1.015 g (2.30 mmol) of $[HNEt_3]^+[B(C_6D_5)_4]^-$ in 15 mL of THT was stirred at room temperature for 2 h, during which time the solution gradually turned yellow and yellow microcrystalline material precipitated. The suspension was warmed until all solids had dissolved, filtered, and slowly cooled to room temperature, depositing large yellow crystals of $[Cp^*_2HfMe(THT)]^+[B(C_6D_5)_4]^-$. Yield: 1.491 g (1.67 mmol, 73%). ^1H NMR (THF-d_8): δ 2.74 (m, 4 H, α-CH_2, free THT), 1.96 (s, 30 H, $C_5(CH_3)_5$), 1.81 (m, 4 H, β-CH_2, free THT), 0.17 (s, 3 H, Hf-CH_3). IR (cm^{-1}): 2728 (w), 2268 (s), 2253 (vs), 1609 (m), 1547 (m), 1520 (s), 1344 (w), 1310 (m), 1262 (s), 1252 (s), 1211 (m), 1202 (m), 1157 (s), 1136 (w), 1084 (m), 1022 (s), 955 (m), 885 (m), 862 (vs), 835 (m), 826 (m), 806 (m), 795 (m), 745 (m), 731 (m), 669 (m), 648 (m), 640 (m), 596 (m), 540 (vs), 517 (m), 475 (m), 453 (m), 422 (vs).

Thermolysis of $[Cp^*_2HfMe(THT)]^+[B(C_6D_5)_4]^-$. A solution of 20.5 mg (0.023 mmol) $[Cp^*_2HfMe(THT)]^+[B(C_6D_5)_4]^-$ in 10 mL of $PhNMe_2$ was degassed on a vacuum line by three freeze–pump–thaw cycles and heated at 55 °C for 2 h. Volatiles were collected by Toepler pump (0.023 mmol, 1.00 equiv) and analyzed by MS. M^+ = 17 (CH_3D, 100%).

X-ray Crystal Structure Determination of $[Cp^*_2ZrMe(THT)]^+[BPh_4]^-$ (1) and $[Cp^*_2HfMe(THT)]^+[BPh_4]^-$ (2). Suitable crystals were grown by slow diffusion of pentane into a concentrated solution of 1 in THT and by slowly cooling a hot, concentrated solution of 2 in THT. The sample crystals were glued on the top of a glass fiber and transferred into the cold nitrogen stream of the low-temperature unit mounted on an Enraf-Nonius CAD-4F diffractometer interfaced to a PDP-11/23 computer. Although for 1 an X-ray structure determination was thwarted by persistent crystal twinning, a successful characterization was executed ultimately with a small, weakly scattering crystal. Unit cell parameters and their standard deviations were determined from a least-squares treatment of the setting angles of 22 reflections in the range $9.07° < \theta < 13.34°$ for 1 and $13.99° < \theta < 17.85°$ for 2 and checked for the presence of higher metrical symmetry.[27] The space group was derived from the observed systematic absences. The crystal system was identified as orthorhombic, space group $Pna2_1$, for both 1 and 2; the E statistics showed unambiguously an acentric space group.[28] This choice was confirmed by the solution and successful refinement in this space group, and examination of the final atomic coordinates of the structures did not yield extra metric symmetry elements.[29] Crystal and/or instrumental instability was monitored by measurement of the intensities of three reference reflections that were collected after every 3 h of X-ray exposure time; there was no indication of crystal decomposition. The net intensities of the data were corrected for the scale variation, Lorentz and polarization effects, and in the case of 2 also for absorption. Standard deviations in the intensities based on counting statistics were increased according to an analysis of the excess variance[30] of the three reference reflections: $\sigma^2(I) = \sigma_{CS}^2(I) + (0.018I)^2$. For 1 this resulted in 2438 reflections satisfying the $I \geq 2.0\sigma(I)$ criterion of observability. To provide an adequate ratio of observations to parameters, only reflections where F_o was less than $2.0\sigma(I)$ were considered unobserved and were not included in the refinement. For 2 empirical absorption corrections based on ($F_o - F_c$) were applied after completion of the isotropic refinement. Correction for absorption was carried out with the program DIFABS,[31] resulting in 3552 reflections satisfying the $F \geq 4.0\sigma(F)$ criterion of observability. The structure of 1 was solved by Patterson methods and subsequent partial structure expansion (SHELXS86[32]). The cell constants of 2 are virtually identical with those of 1. Therefore we assumed that both structures are isomorphous and the coordinates of the non-hydrogen atoms of the zirconium compound were used in the preliminary stage of the refinement of 2 and did refine satisfactorily. The positional and anisotropic thermal parameters for the non-hydrogen atoms were refined with block-diagonal least-squares procedures (XTAL[33]), minimizing the function $Q = \Sigma_h[w(|F_o| - |F_c|)^2]$. At this stage of the refinement

Table VII. Details on the Structure Determination of 1 and 2

	1	2
color	orange/yellow	yellow
chem formula	$C_{49}H_{61}ZrSB$	$C_{49}H_{61}HfSB$
fw	784.11	871.38
cryst syst	orthorhombic	orthorhombic
space group, No.[38]	$Pna2_1$, 33	$Pna2_1$, 33
a, Å	31.31 (1)	31.32 (1)
b, Å	11.844 (4)	11.857 (1)
c, Å	11.084 (4)	11.029 (1)
V, Å^3	4110 (2)	4096 (1)
Z	4	4
D_{calc}, g·cm^{-3}	1.267	1.413
F(000), electrons	1664	1792
μ(Mo Kᾱ), cm^{-1}	4.3	26.0
approx cryst dimens, mm	0.12 × 0.13 × 0.32	0.25 × 0.30 × 0.12
radiation, Å	Mo Kᾱ, 0.710 73	Mo Kᾱ, 0.710 73
monochromator	graphite	graphite
temp, K	130	130
θ range: min, max, deg	1.31, 23.10	1.30, 27.0
ω/2θ scan, deg	$\Delta\omega = 0.70 + 0.35 \tan\theta$	$\Delta\omega = 0.90 + 0.35 \tan\theta$
instability constant, p	0.018	0.019
drift corrcn	0.989–1.031	0.971–1.000
min and max abs corrcn factors		0.69–1.18
total no. of data	3407	5447
no. of unique data	3046	4674
no. of obsd data	2438 ($I \geq 2.0\sigma(I)$)	3733 ($I \geq 4.0\sigma(I)$)
no. of refined params	468	443
final agreement factors:		
$R_F = \sum(\|\|F_o\| - \|F_c\|\|)/\sum\|F_o\|$	0.050	0.055
$R_w = [\sum(w(\|F_o\| - \|F_c\|)^2)/\sum w\|F_o\|^2]^{1/2}$	0.041	0.053
weighting scheme	$1/\sigma^2(F)$	$1/\sigma^2(F)$
$S = [\sum w(\|F_o\| - \|F_c\|)^2/(m - n)]^{1/2}$	1.700	3.002
m = no. of obsns		
n = no. of variables		
residual electron density in final difference Fourier map, e/Å^3	−0.49, 0.58	−1.83, 2.07

(27) Spek, A. L. *J. Appl. Crystallogr.* **1988**, *21*, 578.
(28) Snow, M. R.; Teikink, E.R.T. *Acta Crystallogr., Sect. B* **1988**, *44*, 676.
(29) Le Page, Y. *J. Appl. Crystallogr.* **1987**, *20*, 264.
(30) McCandlish, L. E.; Stout, G. H.; Andrews, L. C. *Acta Crystallogr., Sect. A* **1975**, *31*, 245.
(31) Walker, N.; Stuart, D. *Acta Crystallogr., Sect. A* **1983**, *39*, 158.
(32) *SHELXS86*; Sheldrick, G. M.; University of Göttingen: Göttingen FRG, 1986.
(33) XTAL 2.2 *User Manual*; Hall, S. R., Stewart, J. H., Eds.; Universities of Western Australia, Perth, Australia, and Maryland, College Park, MD, 1987.

of 1, 41 (of 61) hydrogen atom positions could be located on a difference Fourier map. At this stage of the refinement of 2, the hydrogen atom positions of the analogous Zr compound were introduced and refined. The remainder for both 1 and 2 were calculated at idealized geometric positions. Thereby the found hydrogen atoms served to determine the conformation of all methyl groups. All the hydrogen atoms were replaced afterward at idealized positions, by using sp^2 or sp^3 hybridization at the C atom as appropriate and a fixed C–H distance of 1.0 Å. Hydrogen atoms were refined in the riding mode with a fixed C–H bond length of 1.0 Å, given one common fixed isotropic thermal parameter, and used in the structure factor calculations but not refined. Full-matrix least-squares refinement (based on F_o) with anisotropic thermal parameters for the non-hydrogen atoms and one overall temperature factor for the hydrogen atoms converged satisfactorily, giving the corresponding final discrepancy indices summarized in Table VII. Weights were introduced in the final refinement cycles. In the final refinement the nonpositive atoms were returned to isotropic thermal displacement parameters. The polarity of the structures was tested with $i\Delta f''$ and $-i\Delta f''$ values, giving only marginally different R values. For 1 the temperature factors of C12 were nonpositive definite and some atoms showed unrealistic temperature factors, suggesting some degree of disorder, which is in line with the weak scattering power of the crystals investigated. For 2 the temperature factors of C25 were nonpositive definite. In the case of 1, five reflections with $w(||F_o| - |F_c||) > 12$ were excluded from the final refinement cycle. The mismatch could be ascribed to an instrumental error. In the case of 2, a bad agreement ($w(||F_o| - |F_c||) > 10$) was observed for 38 reflections. The mismatch is probably due to a small misoriented fraction of the crystal used in this study. Crystal data and experimental details of the structure determination are compiled in Table VII. Scattering factors were as given by Cromer and Mann.[34] Anomalous dispersion factors, taken from Cromer and Liberman,[35] were included in F_c. All calculations were carried out on the CDC-Cyber 962-31 computer of the University of Groningen with the program packages XTAL,[33] EUCLID[36] (calculation of geometric data), and ORTEP[37] (preparation of illustrations).

Modeling Studies with ALCHEMY II.[22] Potential energy minimization calculations were carried out on the hypothetical cationic species $[Cp^*_2ZrCH_2CH(CH_3)CH_2CH(CH_3)_2]^+$ using geometrical data from the crystal structure of 1 (the THT ligand was omitted and not further taken into account during the calculation), and C–C and C–H bond lengths and angles for the 2,4-dimethylpentyl ligand were taken from data supplied with the ALCHEMY program. For the Cp^*_2Zr moiety, the distance between the metal center and the α-carbon atom of the alkyl ligand was kept fixed, while the α-carbon was confined to the plane symmetrically between the Cp* ligands. To minimize the energy of the ion, the position of the pentyl ligand in the Cp^*_2Zr wedge and bond distances and angles in the pentyl ligand were varied. A conformation with the β-methyl group of the pentyl ligand in the plane between the Cp* ligands (structure A) appeared to be about 4 kcal·mol^{-1} more stable than the conformation with the β-hydrogen atom in that plane (structure B).

Acknowledgment. We thank DSM Research BV for generous financial support of this investigation.

Registry No. 1, 131494-61-6; 2, 131494-63-8; $[Cp^*_2HfMe(THT)]^+[B(C_6D_5)]^-$, 137167-65-8; $Cp^*_2HfMe_2$, 116437-01-5; $[HNEt_3]^+[B(C_6D_5)]^-$, 137167-67-0; C_3H_6, 115-07-1; $(C_3H_6)_2$, 16813-72-2; $(C_3H_6)_3$, 13987-01-4; $(C_3H_6)_4$, 6842-15-5; $(C_3H_6)_5$, 15220-87-8; $(C_3H_6)_6$, 50295-91-5; $(C_3H_6)_7$, 106855-49-6; $(C_3H_6)_8$, 77111-45-6; isobutene, 115-11-7.

Supplementary Material Available: For 1 and 2, tables of fractional atomic coordinates and equivalent isotropic thermal parameters, thermal displacement parameters, bond distances and angles, and torsion angles (24 pages); listings of structure factors (38 pages). Ordering information is given on any current masthead page.

(34) Cromer, D. T.; Mann, J. B. *Acta Crystallogr., Sect. A* **1968**, *24*, 321.
(35) Cromer, D. T.; Liberman, D. *J. Chem. Phys.* **1970**, *53*, 1891.
(36) Spek, A. L. The EUCLID package. In *Computational Crystallography*; Sayre, D., Ed.; Clarendon Press: Oxford, U.K., 1982; p 528.
(37) Johnson, C. K. ORTEP. Report ORNL-3794; Oak Ridge National Laboratory: Oak Ridge Tennessee, 1965.
(38) Hahn, T., Ed. *International Tables for Crystallography*; Reidel: Dordrecht, 1983; Vol. A (space-group symmetry).